GLOBAL JOURNAL OF GEOLOGICAL SCIENCES VOL. 4, NO. 2, 2005: 117 - 132
ISSN 1596-6798. COPYRIGHT BACHUDO SCIENCE CO. LTD. PRINTED IN NIGERIA.

TIME VERSUS FREQUENCY DOMAIN MEASUREMENTS: LAYERED MODEL

N. F. UKAIGWE

(Received 26 September 2002; Revision accepted 19 May 2005)

ABSTRACT

The effect of receiver coil alignment errors δ on the response of electromagnetic measurements in a layered earth model is studied. The statistics of generalized least square inverse was employed to analyzed the errors on three different geophysical applications. The following results were obtained: (i) The FEM ellipiticity is insensitive to orientation error;(ii) The TEM has an error less than 1% for times greater than 0.5 msecs after turn off time. (iii) The standard errors of TEM and FEM for the important parameters of buried conductor models yield approximately the same errors for TEM and FEM data sets; for models with a conductive overburden , the FEM ellipticity gave substantially better parameter errors in comparison with TEM data; and all the data needed less time than the FEM in their high frequency content while among TEM data sets with low frequency content, the averaging times for the FEM ellipticity were shorter than the TEM quality.

KEYWORDS: Ellipticity, Frequency domain, Frequency Electromagnetic method, Model Parameter, Orientation Error, Time domain, Transient Electromagnetic method

INTRODUCTION

The relative merits of time-domain (TEM) and frequency-domain (FEM) electromagnetic field measurements are topics of debate in the geophysical literature. Several new configuration of transmitter-receiver combinations, for use in ground transient electromagnetic surveys, are being investigated in different parts of the world. Prominent among these configurations are (a) one-loop arrangement, (b) displaced loop arrangement, (c) in-loop arrangement, (d) dual loop arrangement (Spies, 1975) , and (e) two-loop arrangement. Pioneering work in this subject is at present being carried out in Australia, at Common wealth Scientific and Individual Research Organization (CSIRO), Mcquarie University and Bureau of Mineral Resources (B.M.R). A matching effort in this subject is the responses observed with receiver coil misorientation in a layered earth. This paper analyzes TEM and FEM soundings calculated numerically over layered earth structures in the presence of:

1. Receiver coil misorientation, and
2. Natural geomagnetic field noise.

MeCracken *et al.*(1980), has considered the problem of coil alignment error on the horizontal(H_r) and vertical (H_z) magnetic fields in both time and frequency domain . A Kaufman(1978a&b) has compared TEM and FEM measurements for closed conductors embedded in resistive host rock using an asymptotic expansions of the fields at early, at late times and low and high frequencies. TEM and FEM measurements are compared in terms of curve separation over layered models by Verma and Mallick(1979).

In this paper, we consider the effects of coil alignment on measured quantities such as $\|H_z(f)\|$, and $\|H_z(f)\|$, as well as on calculated quantities such as total field ellipticity. Our analysis of model parameter resolution uses the statistics of the generalized least squares inverse which is in wide use in layered earth inversion schemes. (Vozoff, 1981). The natural geomagnetic noise spectrum as measured by Labson(1980) is used to provide the TEM and FEM errors.

Three layered models which are representative of geological situations of interest are considered. The first, model A, has an overburden of σ=0.01 S/m, 250 meter thick overlying a σ_2=0.3 S/m basement. Model B with σ_1=σ_3=1.0 S/m, σ_2=0.02 S/m and h_1=h_2=50m was chosen to examine the relative resolving power of TEM and FEM data when conduction overburden masks a conductive basement. The third model, C, has σ_1=σ_3=0.02 S/m σ_2=1.0 S/m, h_1=h_2=50m was chosen to compare TEM and FEM resolution of a thin conductor in resistive host rock.

Receiver Coil Alignment Errors

Figure 1 shows the transmitter-receiver geometry, TEM waveform, and defines the receiver coil misalignment angle δ. In most EM field procedures sensor coils can be aligned to within 0.1 degree of vertical or horizontal. However, the necessity of laying a transmitter loop on uneven ground results in an uncertainty in the direction of the transmitter moment. Thus, one degree of misalignment between transmitter moment and the vertical receiver coil is more reasonable.

The percentage error in the possible measured and calculated TEM and FEM field quantities for model A, σ_1=0.01, h_1 =250m, σ_3=0.3 and T_x-R_x separation of 250m is shown in Figure 2. The frequency band is 1-20,000 hertz and the time-domain interval is 0.5-200m sec. In practice, transient signals later than 50-100m sec after turn-off require more averaging time than is practical in production surveys. However, for this theoretical study later times are used so that the low frequency content of the transient approaches the fundamental frequency of the FEM wave form of equivalent transmitter period.

Figure 2 shows that 1 degree of misalignment produces major errors at some point in either the frequency or time band of all field quantities except one: the total field ellipticity. The maximum error in ellipticity between 1 and 20,000 hertz is 0.002% at 500 hertz.

N. F. UKAIGWE, Department of Geology, University of Port Harcourt, Choba East-West Road, Port Harcourt, Nigeria.

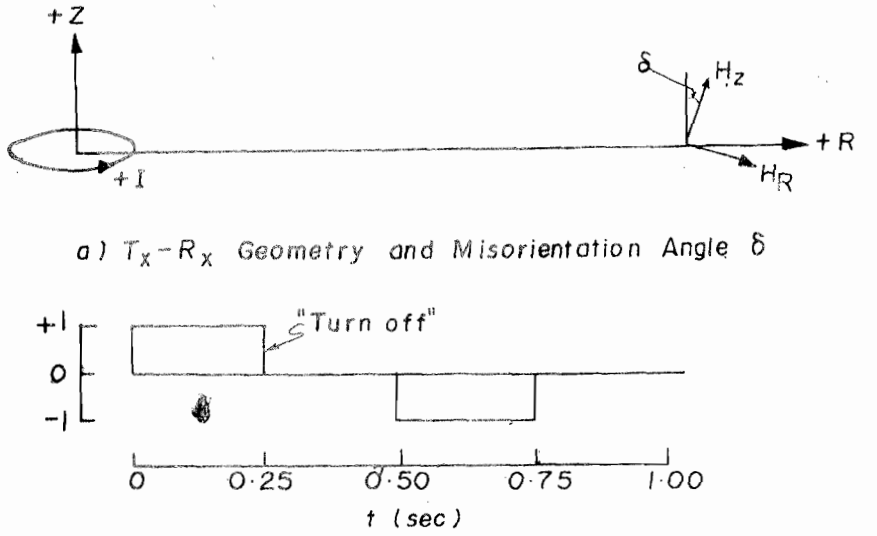

Figure 1 Transmitter geometry and current waveform

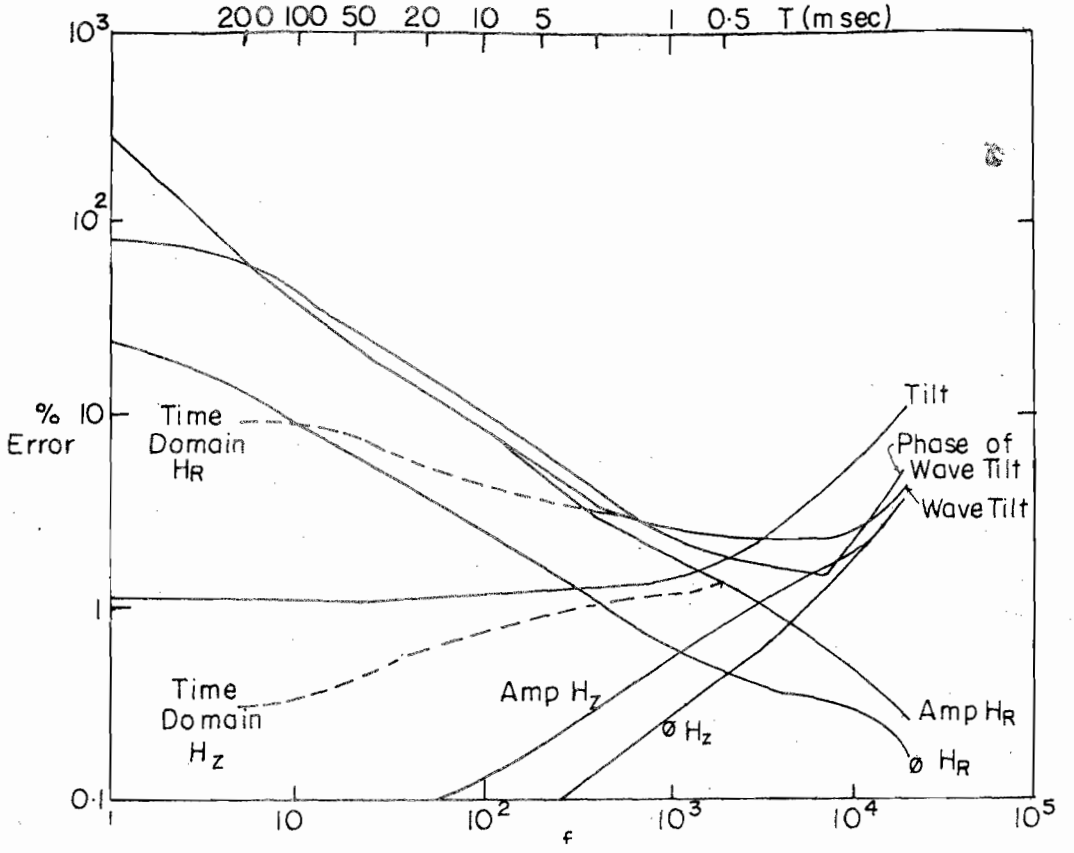

Figure 2 Percent error in field quantities due to 1 degree misorientation of receiver coil.

This accuracy for ellipticity assumes that the H_z and H_R coils are orthogonal, as could be obtained in a permanently mounted pair of coils.

The error induced in the transient H_z and H_R responses should be noted since it is often incorrectly assumed that measuring in the "off-time" causes coil orientation errors to become negligible. (Lee 1982; Lee and Lewis 1974, Buselli 1974)As Figure 2 shows, the error in $H_R(t)$ approaches 10% at late times and is never better than 2% in the interval(0.5-200m sec). However, at times less than 1msec the error exceeds 1%.

Among the FEM field quantities ellipticity is clearly the least sensitive to orientation provided the two measuring coils are orthogonal. For TEM measurements $H_z(t)$ is the least sensitive to orientation . It seems natural that a measurement of $H_{total}(t)$ by

two orthogonal coils in the time-domain would result in misalignment errors comparable to ellipticity measurements in the frequency-domain. For a plot of total H as a function of time see Hoversten and Morrison (1981).

Statistics of the Generalized Least Square Inverse

The theory of the generalized least squared inverse as applied to EM and DC resistivity soundings is well described by Glenn (1973) and Inman (1975), respectively. For this study we will consider the model parameter standard errors, S_i, I=1, M where M is the number of parameters, the parameter correlation coefficients C_{ij} i=1, M,j=1, M, and the information density matrix. The parameter standard errors and correlation coefficients are used to evaluate the model resolution of different TEM and FEM data sets. The information density matrix, D, is used to check the information distribution of the data sets to insure the quantities S_i and C_{ij} i=1, M are not biased by improper data sampling.

The parameter standard errors, S_i, are related to the observed data and iterated model through the system matrix, A, where:

$$A_{ij}=\frac{\partial \Delta C_i}{\partial P_j}$$

where

C_i=ith calculated data

P_j= jth model parameter j=1,Nφ

Once the iterative least squares algorithm reaches the minimum value of $\Delta G_{min}=\sum_{i=1}^{N}\left(\frac{\Delta G_i}{\sigma_i}\right)^2$

where $G_i=\{O_i-C_i\}$I=1,N

and σ_i= the measured error of the ith data the model parameter of the standard errors are calculated from

$$S_i=\sqrt{v_{ii}}$$

Where

$$V=\hat{\sigma}^2\left(A^T\ w^{-1}A\right)^{-1}$$

$$\hat{\sigma}^2=\sum_{i=1}^{N}\frac{\left(\Delta G_i\right)^T w^{-1}\Delta G_i}{N-M}$$

$$w_{ij}=\begin{cases}\sigma_i^{\,2} & i=j\\ 0 & i\neq j\end{cases}$$

For a description of the parameter correlation coefficients, see Ukaigwe (1998; Chapter 7).

Therefore, by considering the standard deviations in conjunction with parameter correlations a more realistic parameter standard deviation can be arrived at which is always less than or equal to the standard deviation computed from equation (2).

The information density matrix, D, is defined at the minimum sum of squares AG_{min} as $\underset{(N\times M)}{D}=\underset{(N\times M)}{A}\ \underset{(M\times N)}{H}$ where H is the generalized inverse of A. The reader is referred to Glenn and Ward (1976) and Ward *et al.* (1976) for a detailing description of D and its uses.

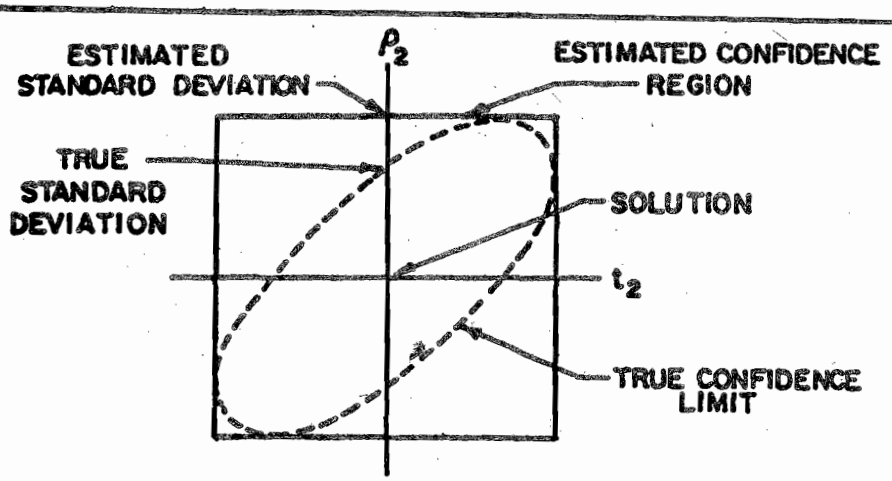

Figure 3: Generalized slice of solution space, after Inman 1975

Briefly, the information density matrix has the dimensions of the data, (N×N). The diagonal elements of D have peaks in the range (0,1) at locations, which correspond to data that contribute the most in determining the model through the least squares inverse. Large off diagonal elements indicate an inter-relationship between data. Table 1 presents the data numbers and their corresponding times and frequencies.

The model parameter standard errors and correlation coefficients are used to compare the resolution of various field quantities under the following assumptions:

1. There are equal number of TEM and FEM data; and
2. All data have been averaged to reach a 1 percent error.

In order to evaluate the effect of data sampling on parameter standards errors, an arbitrary sampling scheme was chosen for both FEM and TEM sampling. The arbitrary FEM sampling, equispaced points in $\log_{10}$ space, is given by:

$$\Delta_F = \frac{\log_{10}[\text{freq}(N)] - \log_{10}[\text{Freq}(1)]}{N-1} \quad .. \quad .. \quad .. \quad 4$$

$$\text{Freq}(I) = {}_{10}(\log_{10}\text{Freq}(1) + (I-1)\,\Delta_F)\ ;\ I=I,N \quad .. \quad .. \quad ..$$

The arbitrary TEM sampling is given by:

$$\Delta_T = \frac{\log_{10}[\text{Time}(N)] - \log_{10}[\text{Time}(1)]}{N-1} \quad .. \quad .. \quad .. \quad 5$$

$$\text{Time}(I) = {}_{10}(\log_{10}\text{Time}(I) + (I-1)\,\Delta_T)\quad I=I,N$$

TABLE 1: Data numbers and their corresponding times and frequencies

	Frequency Equation 2		Time Equation 3		Frequency Set #2		Time Set #2	
	1-2000 Hz	25-20,000 Hz	0.05-9 sec	0.05-200m sec	1-2000 Hz	25-20,000 Hz	25-20,000 Hz	0.05-9m sec
1.	1.0	25.0	0.050.05	0.5	1.0	25.0	0.05	0.5
2.	1.49	35.0	0.390.39	8.3	2.0	31.5	0.1	1.0
3.	2.2	60.5	0.750.75	16.1	3.5	50.0	0.15	1.5
4.	3.32	71.8	1.11	24.7	4.0	80.0	0.2	2.0
5.	4.95	102.12	1.49	33.1	6.3	100.0	0.25	2.5
6.	7.4	145.1	1.88	42.2	8.0	125.0	0.3	3.0
7.	10.0	206.4	2.29	51.4	10.0	200.0	0.4	5.0
8.	16.45	293.4	2.71	60.8	16.0	315.0	0.5	7.0
9.	24.54	417.2	3.14	70.57	20.0	400.0	0.7	10.0
10.	36.6	593.0	3.60	80.6	31.5	500.0	1.0	15.0
11.	54.6	843.1	4.05	90.9	40.0	800.0	1.5	20.0
12.	81.5	1198.6	4.53	101.6	80.0	1000.0	2.0	25.0
13.	121.58	1704.0	5.02	112.6	100.0	1250.0	2.5	30.0
14.	181.38	2422.5	5.54	124.0	125.0	2500.0	3.0	35.0
15.	270.6	3444.0	6.07	135.7	200.0	4000.0	4.0	40.0
16.	403.7	4896.1	6.62	147.8	400.0	5000.0	5.0	50.0
17.	602.3	6960.6	7.18	160.2	500.0	6300.0	6.0	75.0
18.	898.6	9895.6	7.77	163.1	800.0	10000.0	7.0	100.0
19.	1340.5	14068.1	8.37	176.4	1000.0	12500.0	8.0	150.0
20.	2000.0	20000.0	9.0	200.0	2000.0	20000.0	9.0	200.0

The samplings provided by equations (4) and (5) were analyzed using the information density matrix, D, evaluated for the three models used in this paper.

Figure 4 shows D, the parameter correlation coefficients $C_{i,j}$, and the parameter standard errors of $H_R(t)$ for times in the range 0.5-200msec over model A with equation (5) used to calculate the time samples. In figure 4 there is a high concentration of contours at early times and a lack of relief at the mid times. This indicates that the early times picked by using equation (5) contain more useful information than the mid-times. Thus, a better sampling would concentrate data in the time interval with high relief in D, Figure 4 (early times), and sample less densely in the mid-times where D showed little relief. A new time sampling, denoted "time set 2," was chosen as described above which resulted in the information density matrix shown in Figure 5. The information is now more evenly distributed over the data set, indicating that ellipticity (1-2000 hertz) and shows an even distribution of information over the data set, indicating that equation (4) provides a good sampling interval for FEM measurements. In the later analysis where parameters are taken from the EM-60, Morrison *et al* (1978), the frequencies were picked to coincide with actual filter settings which were chosen as close to values from equation (4) as possible. The second frequency sampling, denoted "frequency set 2" was also checked using D and showed little change from the sampling provided by equation (4).

Table 2 presents S_i for FEM and TEM quantities. For model A the S_i for ellipticity $H_z(t)$ and $H_R(t)$ for both sampling sets are shown for comparison. Both FEM sets provide approximately equal Si while TEM set 2 yields improved h_1 standard errors.

The model A results of Table 2 show that among the FEM quantities, amplitude of H_R and ellipticity provide the best overall model resolution. Considering the susceptibility of $|H_R|$ to sensor orientation, elllipticity is the only FEM quantity with low sensor orientation sensitivity and good parameter resolution. The TEM quantities H_z (t) and H_R (t) have approximately equal parameter errors but the sensitivity to coil alignment of H_R (T) leaves H_z (t) as the most desirable TEM quantity.

A comparison of the correlation coefficient given in Figure 5 and 6 shows that ellipticity generally produces lower correlation between parameters than does H_R (t). This is also true of a comparison between ellipticity and H_z (t) for model A.

FINAL MODEL PARAMETERS

PARAMETER NO. 1 = 1.000E+02	STANDARD ERROR = 2.111E +00
PARAMETER NO. 2 = 2.500E+02	STANDARD ERROR = 1.571E +00
PARAMETER NO. 3 = 3.333E+00	STANDARD ERROR = 1.493E +00

PARAMETER CORRELATION MATRIX

	RES1	THK1	RES2
RES1	1.00	-.67	.54
THK1	-.67	1.00	-.91
RES2	.54	-.91	1.00

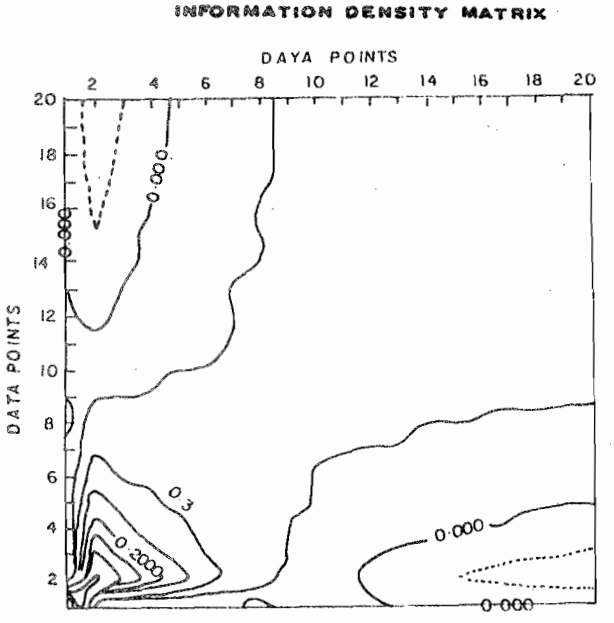

Figure 4 Information density matrix, parameter standard errors and correlation and Coefficients for H_r for model A, time interval 0.5-200 msec with sample times calculated.

FINAL REPORT MODEL

PARAMETER NO. 1 = 1.000E+02 STANDARD ERROR = 1.850E +00
PARAMETER NO. 2 = 2.500E+02 STANDARD ERROR = 7.470E -01
PARAMETER NO. 3 = 3.333E+00 STANDARD ERROR = 1.251E - 02

PARAMETER CORRELATION MATRIX

	RES1	THK1	RES2
RES1	1.60	-..55	.35
THK1	-.65	1.00	-.76
RES2	..35	-.76	1.00

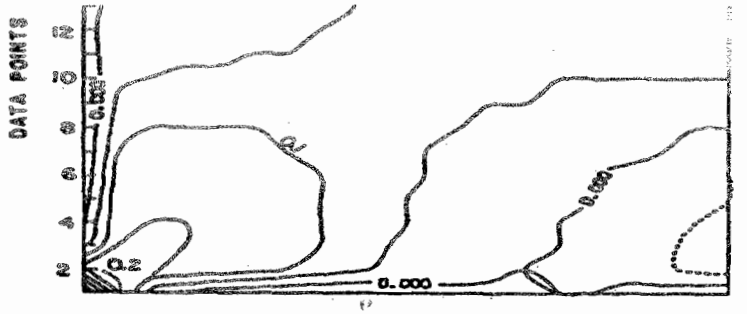

Figure 5: Information density matrix, parameter standard errors, and correlation coefficients for H_r for model A, 00msec.(time set 2).

FINAL MODEL PARAMETER

PARAMETER NO. 1 = 1.000E+02 STANDARD ERROR = 5.770E +00
PARAMETER NO. 2 = 2.500E+02 STANDARD ERROR = 1..5686E -01
PARAMETER NO. 3 = 3.333E+00 STANDARD ERROR = 5..9986E- 02

PARAMETER CORRELATION MATRIX

	RES1	THK1	RES2
RES1	1.00	-..55	.28
THK1	-.45	1.00	-.88
RES2	.28	-.98	1.00

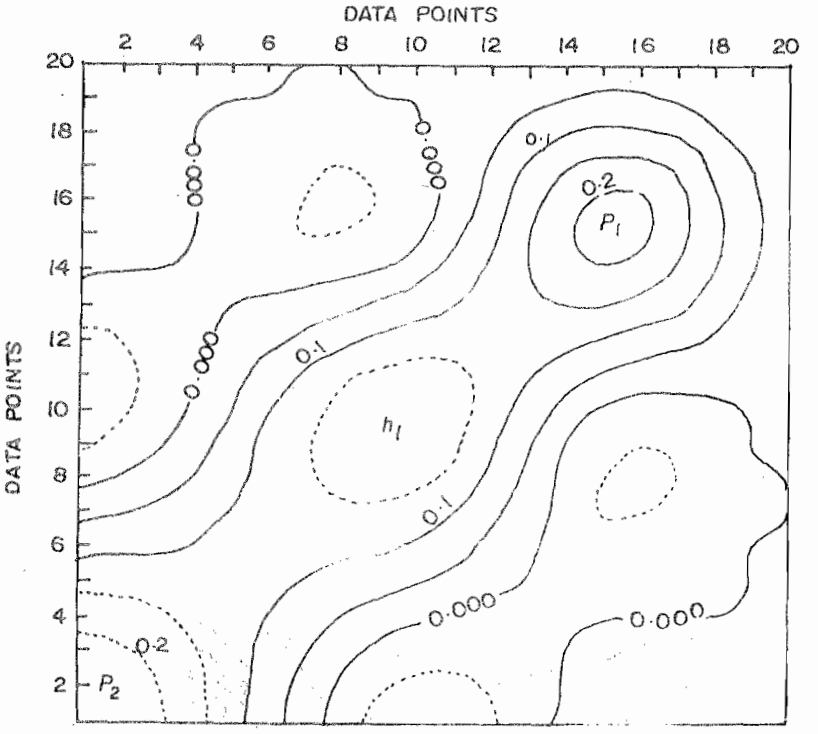

Figure 6 Information density matrix, parameter standard errors, and correlation coefficients for ellipticity in frequency band 1-2000 hertz with sample frequencies calculated by Equation. 4.

The model standard errors for model B show that both the FEM and TEM measurements resolve the upper and lower conductivities equally well. However, the ellipticity produced substantially lower $S_i^{(s)}$ for h_1,σ_2, and h_2, than did either $H_R(t)$ or $H_z(t)$. The increased uncertainty of parameters exhibited by the TEM data compared to FEM data also manifests itself in the correlation coefficients given in Table 3. In general, the TEM correlation coefficients are much larger than their FEM counterparts. In particular, note the high correlation between ,σ_2 and h_2 for all TEM data sets compared to the FEM correlations between σ_2 and h_2.

Tables 2 and 3 indicate superior parameter resolution for ellipticity compared to H_R (t) or H_z (t) and, among TEM data $H_R(t)$ is superior to $H_z(t)$ in producing small $S_i^{(s)}$ and $C_{ij}^{(s)}$ for model B.

An initial concern when making this comparison is that the TEM sampling provided by time set 2 somehow biases the parameter resolution. In order to check this an alternative TEM data set was chosen using D calculated for model B using set 2. Figure 7 shows D for model B with the peaks labeled according to the parameters most affected by the data with the corresponding number.

Using D from Figure 7, a set data from 0.5-40 msec was chosen so that sampling concentrated around times which corresponded to peaks in D. This alternate set did not improve the parameter standard errors or correlation coefficients listed in Table 2. From this we conclude that the TEM $S_i^{(s)}$ listed in Table 2 for model B are not unfavorably affected by the TEM data sampling and are an accurate representation of the parameter resolution provided by TEM data for model B.

In the case of a thin conductor embedded in a resistive host, model C, the standard errors of the most important parameters, h_1, σ_2 & h_2 are essentially equal for FEM and TEM measurements.
The ellipticity gives a large S_{h_1} on σ_3 and both H_z (t) and H_R (t) yield large errors on σ_1. The parameter correlations for model C are given in Table 4 and as was the case for model B, the TEM $C_{i,j}^{(s)}$ are in general larger than FEM counterparts. The TEM correlations between σ_2 and h_2 are again much larger than those for the FEM data.

From the results presented in Tables 2, 3, and 4, it is apparent that FEM ellipticity provides parameter resolution which is as good as (model A) or better than (models B and C) that provided by either TEM data set.

TABLE 2: Model A: Equations 2&3, Time & Frequency Set 2

Equation 2(1-2000 hz)

	ρ_1	h_1	ρ_2
$\lvert H_z \rvert$	5.7	13.7	0.9
ϕ_z	4.5	48.5	3.8
$\lvert H_R \rvert$	0.6	1.6	0.06
ϕ_R	4.8	7.9	0.3
Ellipt.	0.7	1.8	0.07
Tilt	1.8	22.0	1.9

Frequency Set 2 (1-2000 hz)

ρ_1	h_1	ρ_2
0.06	1.6	0.06

Equation 3(0.5-200msec)

$H_z(t)$	2.3	1.9	0.02
$H_R(t)$	2.1	1.6	0.01

Time Set 2

2.2	1.0	0.02
1.8	0.7	0.01

Model B: Time & Frequency Set 2

(1-2000 Hz, 0.5-200 m sec)

	ρ_1	h_1	ρ_2	h_2	ρ_3
Ellip.	.007	1.2	114.8	3.7	.06
$H_z(t)$	0.03	3.6	734.1	13.7	.01
$H_R(t)$	.002	5.3	615.0	11.7	.009

(1-20,000 Hz, 0.5-200 m sec)

ρ_1	h_1	ρ_2	h_2	ρ_3
.005	1.7	87.8	11.0	0.3
.0	10.3	1176.0	30.9	.08
.009	3.7	521	12.7	.08

Model C: Time & Frequency Set 2

Ellip	0.9	0.3	0.01	1.5	40.0
$H_z(t)$	29.9	1.2	0.02	1.5	1.4
$H_R(t)$	68.3	3.3	.04	2.5	1.3

0.5	0.2	.01	2.2	108.4
1.5	0.4	.01	1.8	80.0
6.7	0.9	.05	4.7	106.0

TABLE 3 Model B: Correlation Coefficients

FEM

(1-2000 Hz)

	ρ_1	h_1	ρ_2	h_2	ρ_3
ρ_1	1.0	-.35	.77	.50	-.03
h_1		1.0	.78	.23	-.58
ρ_2			1.0	-.33	-.15
h_2				1.0	-.83
ρ_3					1.0

(25-20,000 Hz)

	ρ_1	h_1	ρ_2	h_2	ρ_3
ρ_1	1.0	-.10	-.63	.16	-.01
h_1		1.0	.36	.83	-.78
ρ_2			1.0	-.18	-.11
h_2				1.0	-.95
ρ_3					1.0

TEM

(0.5-200 m sec Hz)

	ρ_1	h_1	ρ_2	h_2	ρ_3
ρ_1	1.0	-.81	.94	.94	-.50
h_1		1.0	.96	.94	-.32
ρ_2			1.0	-.10	-.45
h_2				1.0	-.53
ρ_3					1.0

(0.05-9m sec Hz)

	ρ_1	h_1	ρ_2	h_2	ρ_3
ρ_1	1.0	-.93	-.98	.98	-.16
h_1		1.0	.98	.94	-.07
ρ_2			1.0	-.99	-.09
h_2				1.0	-.26
ρ_3					1.0

TEM

(0.5-200 m sec H_R)

	ρ_1	h_1	ρ_2	h_2	ρ_3
ρ_1	1.0	0.09	-.2	.17	-.26
h_1		1.0	.94	-.92	.06
ρ_2			1.0	-.99	.15
h_2				1.0	-.23
ρ_3					1.0

(0.05-9m sec H_R)

	ρ_1	h_1	ρ_2	h_2	ρ_3
ρ_1	1.0	-.46	-.60	.50	-.31
h_1		1.0	.91	.74	-.26
ρ_2			1.0	-.94	-.60
h_2				1.0	-.83
ρ_3					1.0

TABLE 4

Model C: Correlation Coefficients

FEM

(1-2000 Hz)

	ρ_1	h_1	ρ_2	h_2	ρ_3
ρ_1	1.0	-.34	.39	.22	-.07
h_1		1.0	-.44	-.41	-.31
ρ_2			1.0	.71	.21
h_2				1.0	-.81
ρ_3					1.0

(25-20,000 Hz)

	ρ_1	h_1	ρ_2	h_2	ρ_3
ρ_1	1.0	.65	.31	.22	.26
h_1		1.0	-.09	.10	-.27
ρ_2			1.0	-.35	-.14
h_2				1.0	-.93
ρ_3					1.0

TEM

(0.5-200 m sec H_R)

	ρ_1	h_1	ρ_2	h_2	ρ_3
ρ_1	1.0	-.99	-.89	-.94	.42
h_1		1.0	.96	-.98	-.48
ρ_2			1.0	.99	.56
h_2				1.0	.60
ρ_3					1.0

(0.05-9 m sec H_R)

	ρ_1	h_1	ρ_2	h_2	ρ_3
ρ_1	1.0	-.01	.44	.15	-.29
h_1		1.0	.11	-.94	-.87
ρ_2			1.0	-.16	-.53
h_2				1.0	.92
ρ_3					1.0

TEM

(0.5-200 m sec H_R)

	ρ_1	h_1	ρ_2	h_2	ρ_3
ρ_1	1.0	-.96	.71	.87	-.16
h_1		1.0	-.86	-.96	-.02
ρ_2			1.0	-.97	.44
h_2				1.0	.28
ρ_3					

(0.05-9 m sec H_R)

	ρ_1	h_1	ρ_2	h_2	ρ_3
ρ_1	1.0	-.39	.26	.41	.46
h_1		1.0	-.90	-.67	.32
ρ_2			1.0	.86	-.53
h_2				1.0	.88
ρ_3					

FINAL MODEL PARAMETERS

PARAMETER NO.1 =1.000E+00	STANDARD ERROR= 2.693E- 02
PARAMETER NO.1 =5.000E+01	STANDARD ERROR= 3.693E+00
PARAMETER NO.1 =5.000E+01	STANDARD ERROR= 7.341E+02
PARAMETER NO.1 =5.000E+01	STANDARD ERROR= 1.375E+01
PARAMETER NO.1 =5.000E+00	STANDARD ERROR= 1.397E- 02

PARAMETER CORRELATION MATRIX

	RES1	THK1	RES2	THK2	RES3
RES1	1.00	-.81	-.94	.94	-.50
THK1	-.21	1.00	.96	-.94	..32
RES2	-.94	.96	1.00	-1.00	.45
THK2	.94	-.94	-1.00	1.00	-.53
RES3	-.50	.32	.45	-.53	1.00

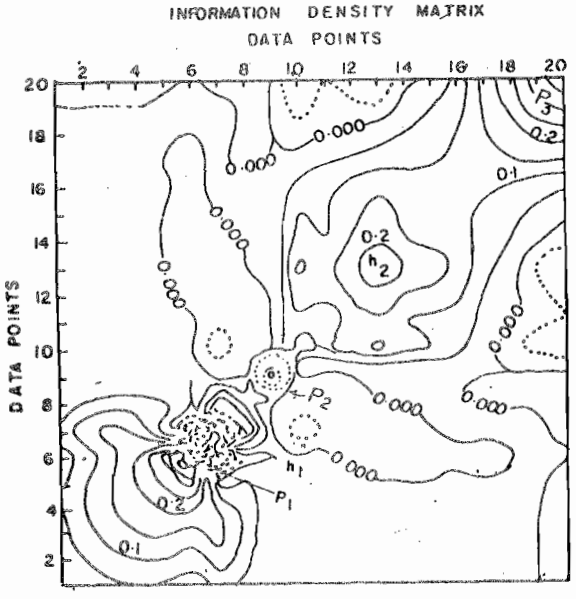

Figure 7 Information density matrix, parameter standard errors, and correlation coefficients for H_z in time interval 0.5-200msec.(time set 2).

The comparison of FEM and TEM data now centers on the following question: given a measured natural field noise spectrum, and its equivalent time series variance, to derive errors on calculated FEM and TEM data respectively, what is the averaging time needed to reach a given percent error on all data in the two domains?

Statistical Basis for Use of Natural Field Spectrum as Noise

From Bendat and Piersol(1971) the variance of time series is

$$\sigma^2_x = \Psi^2_x - \mu^2_x \quad \ldots \quad \ldots \quad 6$$

where

$$\Psi^2_x = \lim_{T\to\infty} \frac{1}{T} \int_0^T x^2(t)dt$$

$$\mu^2_x = \lim_{T\to\infty} \frac{1}{T} \int_0^T x(t)dt$$

We will assume that for the geomagnetic noise $\mu^2_x=0$. From Bendat and Piersol (1971):

$$\frac{\psi_x^{\,2}(f,B_e)}{B_e} = G_x(f) \quad \ldots \quad \ldots \quad 7$$

where $G_x(f)$ is the power spectrum of x(t) and B_e is the bandwidth of the measuring device. Figure 8 presents the amplitude spectrum of the Horizontal magnetic field $\left(\overline{G(f)}_H \right)$ per square root of frequency from 1 to 25,000

hertz taken from Labson (1980). Since $\left(\sqrt{G(f)}_H\right)$ is per square root of frequency, picking $\left(\sqrt{G(f)}_H\right)$ from figure 8 yields the standard deviation directly, where the standard deviation $\sigma^2_x(f)$ is given by:

$$\sigma_x(f)=\Psi^2_x(f)=\sqrt{G(f)}_H \quad .. \quad .. \quad 8$$

In field operation the signal is passed through a tuneable filter notched at the operating frequency. The bandwidth of the notched filter would then become B_e in equation (7) so that when the effects of a filter are considered:

$$\sigma_x(f)=\sqrt{G(f)}\times\sqrt{B_e(f)} \quad .. \quad .. \quad 9$$

For the time domain error we make use of equation (6.83, p.186. Bendat and Piersol (1971), the mean square value of x(t) between any two frequencies f_1 and f_2 is:

$$\Psi^2_x(f_1,f_2)=\int_{f_1}^{f_2} G_x(f)dt \quad .. \quad .. \quad 10$$

Equation (10) was used to calculate $\sigma_x(f_1,f_2)=\Psi^2_x(f_1,f_2)$ where $f_1=1$ and f_2 = 25,000 hertz. Using equation (10) as the error on the transient signals assumes that transients are low passed at $f_2= 2.5\times10^4$ hertz and high passed at $f_1= 1$ hertz.

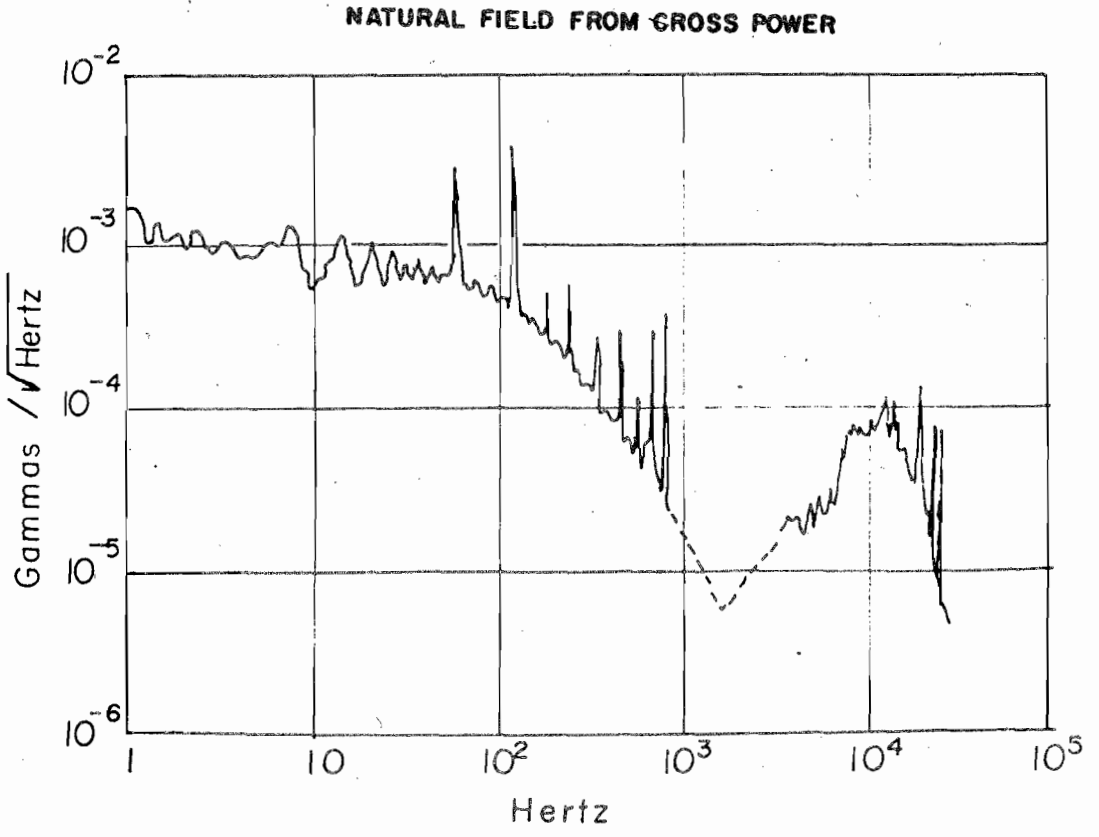

Figure 8 Natural field noise spectrum from Labson (1980)

In the analysis to follow, all parameters such as filter bandwidths, transmitter moment as a function of frequency, and time domain sampling interval are taken from the LBL EM-60 system, Morrison *et al* (1978).

To calculate the FEM error bars we assumed that $\| G(f)_{vertical} \| \approx \| G(f)_{horizontal} \|$ and that vertical components were uncorrelated. This might be considered as a worst case since $\| G(f)_v \| \approx 1 \| G(f)_h \|$ A normally distributed random number generator with zero mean and variance equal to $(\sqrt{G(f)}\times\sqrt{B_e(f)})$ was used to add to the calculated real and imaginary H_z and H_R components, these were then combined to form the calculated FEM quantities. This operation was performed until the calculated variances of each quantity asymptoted to a constant value. The asymptotic value was then taken as the variance on each calculated field

quantity such as ellipticity. The number of periods of the transmitter needed to average the variances to 1% of the known field quantity was calculated. For the TEM data is straightforward, but the number of periods needed for the TEM data depends on both averaging window width and sampling interval within each window.

The number of samples per window was determined by the equation (11)

$$NS_i = 2 \times n_{min} + 1 \quad .. \quad .. \quad .. \quad 11$$

where:

N = number of data(20)
Δ = sampling interval (40 μ sec)
T_i = time of transmitter turnoff
T_1 = center time of (i-1)th window i=2, N + 1
NS_i = number of samples for nth window
$n_i = (Ti-T_{1-1})/\Delta$
$n2 = (T_{i+1}-T_i)/\Delta$
n_{min} = Minimum (n_1 , n_2)

If NS_i is the number of samples per ith window and NW_i is the number of ith windows averaged and Σ_1 is the square root of equation (10), then the error of the average from the ith window is given as Σ_1 = $\Sigma_1 / \sqrt{NS_i}$ and the error after NW_i window have been averaged is Σ_1 total = $\sqrt{NW_i}$

For a given Σ_1 and a chosen Σ_1 total, (1% in this case)

$$\left(\frac{S_i}{\sum_1 total}\right)^2 = \left(\frac{\sum_i}{\sum_1 total}\right)^2 \frac{1}{NS_i}$$

So the number of windows needed is inversely proportional to the number of samples per window. The time necessary to reach Σ_1 total = 1% of the ith averaged field value using two transmitter per period is T=(wave form period ×NW)/2. The times quoted for the TEM data are for 1% or better on all windows since by the time the noisiest window reaches 1% error all other errors are less than 1%.

Averaging Times for TEM and FEM Data

The times, in seconds, needed to average all data to 1 percent or better for the three models considered are given in Table 5. The transmitter receiver separation is 250m and the transmitter moment(NIA) is 10^5. For the FEM data the transmitter current (moment), is frequency dependent due to the induction and capacitance of the transmitter loop. The LBL EM-60 transmitter current decreases approximately linearly with frequency above 1 hertz. For this study the transmitter current is assumed to decrease from 100 amps at 1 hertz to 1 amp to 1000 hertz. The current is assumed to be 1 amp at frequencies above 10^3 since most high frequency systems tune the transmitter for maximum current at a given frequency.

Time for S/N>100 on all Data
NIA=10^5, R=250m

TEM Data

Figure 9 presents $H_R(t)$ or the (0.05-9)m sec time interval, the square root of the TEM variance equals 7.8×10^3 gammas and is shown as a dashed line on the figure. For the TEM data sets the time required to average the noise on all windows to less than or equal to a given percentage of the signal is controlled by two factors:

1. the signal to noise ratio, S/N of the noisiest averaging window; and
2. the number of samples taken sample window.

The number of sample window as determined by equation (11) are listed in Table 6. It will be useful to define the net signal to noise ratio of the ith window as

$$(S/N)^i_{net} = (S/N)^i \times \sqrt{NS_i} \quad .. \quad .. \quad .. \quad 12$$

For $H_R(t)$0.5-9m sec model C requires the least averaging time and model B requires the most.
The short time required for the model C is apparent in figure 9 since the worst $(S/N)_{net}$ occurs for the 20th window where

$$(S/N)^{20}_{C}net = 10.3\times7 = 72.1$$

Recalling that two transients are stacked per wave form period, only a single 40 msec period is needed for model C.

The difference in averaging times for models A and B is illustrative of the effect of the number of samples
In the noisiest window. Upon first inspection of Figure 9 one might expect the averaging time for model B to be less than that of model A. The noisiest window for model B is #7 with S/N = 0.59. However, the zero crossing between 0.3 and 0.4msec in $H_R(t)$ for model B causes the lowest S/N window to be one of the early time windows with only a few samples. For model A the lowest S/N occurs in the last window where 49 samples are taken. The resulting net signal to noise ratios are:

$$(S/N)^{7}_{B}net = 1.65\times\sqrt{5} = 3.64$$

$$(S/N)^{20}_{A\,net} = 0.59\times\sqrt{49} = 4.13$$

The net signal to noise ratios of the noisiest windows for models A and B reveal why model A requires less time, fewer periods, than model B to reach 1% or better errors on all windows.

The HZ(t) transient for the 0.05-9msec interval are shown in figure 10. The net signal to noise ratios for the noisiest windows are:

$$(S/N)^{13}_{C\,net} = 3.62\times\sqrt{25} = 18.1$$

$$(S/N)^{1}_{A\,net} = 3.42\times\sqrt{3} = 5.92$$

$$(S/N)^{17}_{B\,net} = 0.706\times\sqrt{49} = 4.94$$

These are the $(S/N)^{i}_{net}$ which determine the times in Table 5.
The $H_R(t)$ and $H_z(t)$ late time transient, 0.5-200msec, are shown to Figures 11 and 12, respectively. The averaging times for these signals are determined by the low S/N of the latest time windows. Therefore, the order of the averaging times from small to large is the same as the order of the amplitudes at 200msec, namely B,A,C.

Because field systems rarely record transients later than 50 msec after turn off the averaging times for data out to 50msec is included in Table 5. It should be remembered, however, that these data sets do not contain the low frequency present in FEM data for the same transmitter period.

TABLE 5

	Model A	Model B	Model C
H_R(0.05-9m sec)	11.64	10.08	0.04
H_z(0.05-0m sec)	5.68	8.18	1.78
H_R(0. 5-200m sec)	11227.0/456.5	41.5/.5	1.7306/206.5
H_R(0. 5-200m sec)	257.5/31.5	3.5/.5	6548.0/20.5
Ellip.(1-2000 H_z)	1914.9	91.11	32.81
Ellip.(25-20,000 H_z)	29.9	11.27.12	14.63

TABLE 6: Number of Sample Windows

(0.05-9 msec)	
Window #	# of Samples
1	3
2	3
3	3
4	3
5	3
6	3
7	5
8	5
9	15
10	25
11	25
12	25
13	25
14	25
15	49
16	49
17	49
18	49
19	49
20	49

(0.05-200 msec)	
Window #	# of Samples
1	25
2	25
3	25
4	25
5	25
6	25
7	99
8	99
9	149
10	249
11	249
12	249
13	249
14	249
15	249
16	499
17	1249
18	1249
19	2499
20	2499

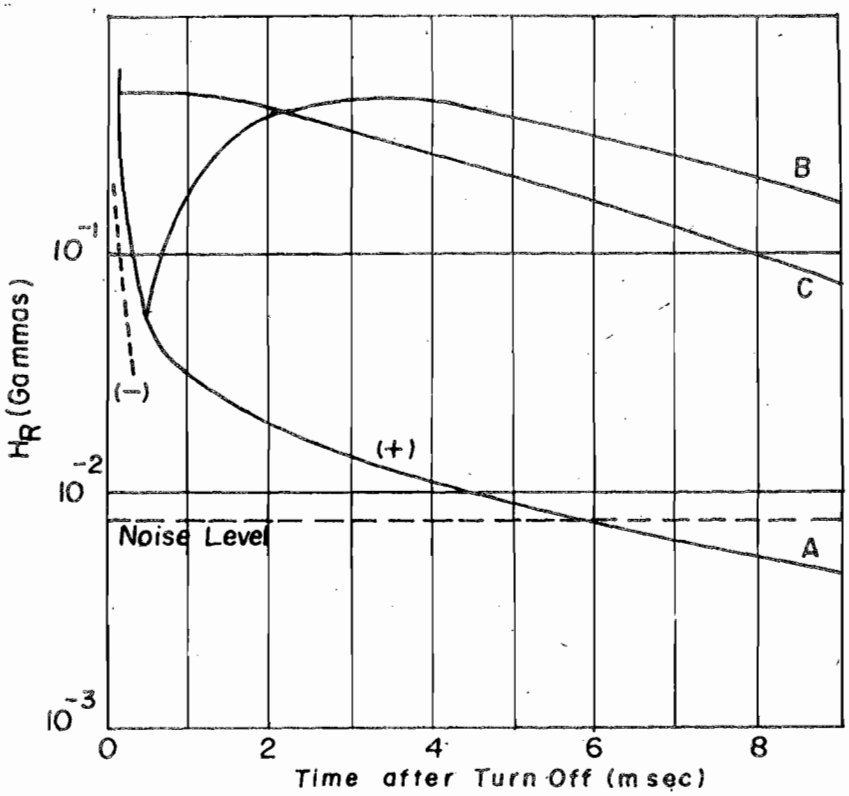

Figure 9 H_r (t) 0.05-9.0 msec time interval.

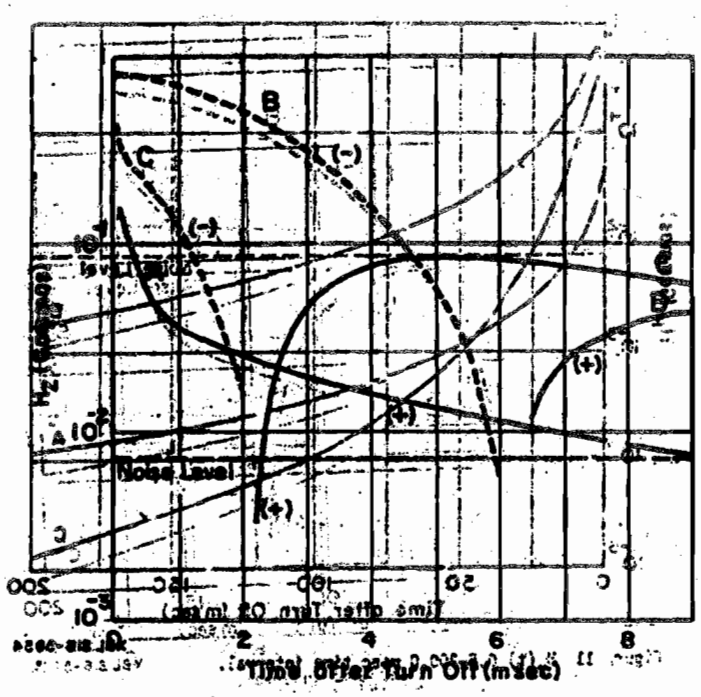

Figure 10 Hz(t) 0.05-9.0 msec. Time interval.

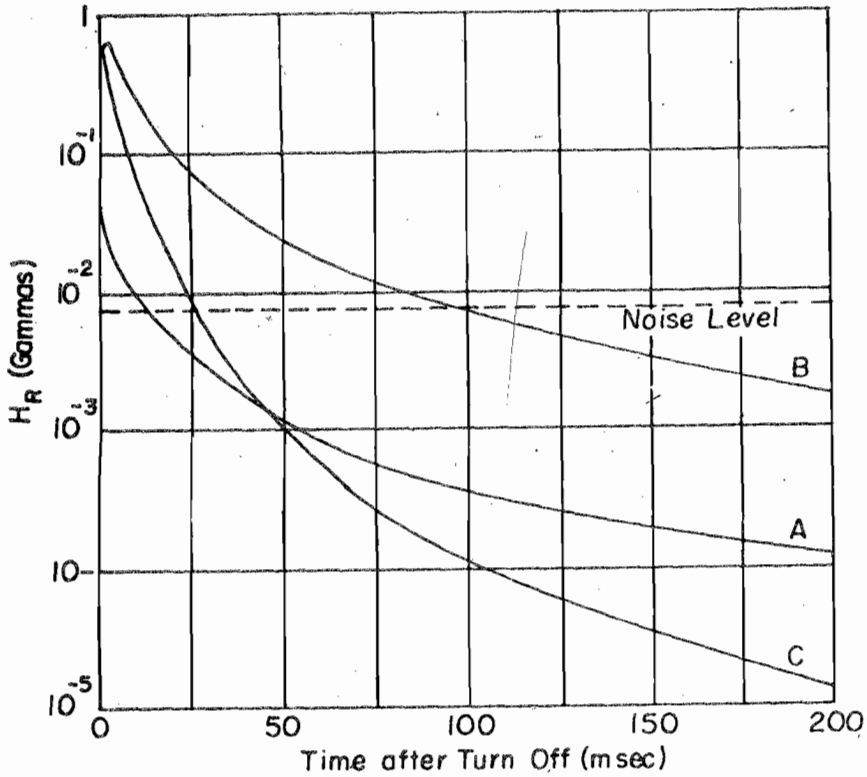

Figure11 H_r (t) 0.05-200.0 msec time interval

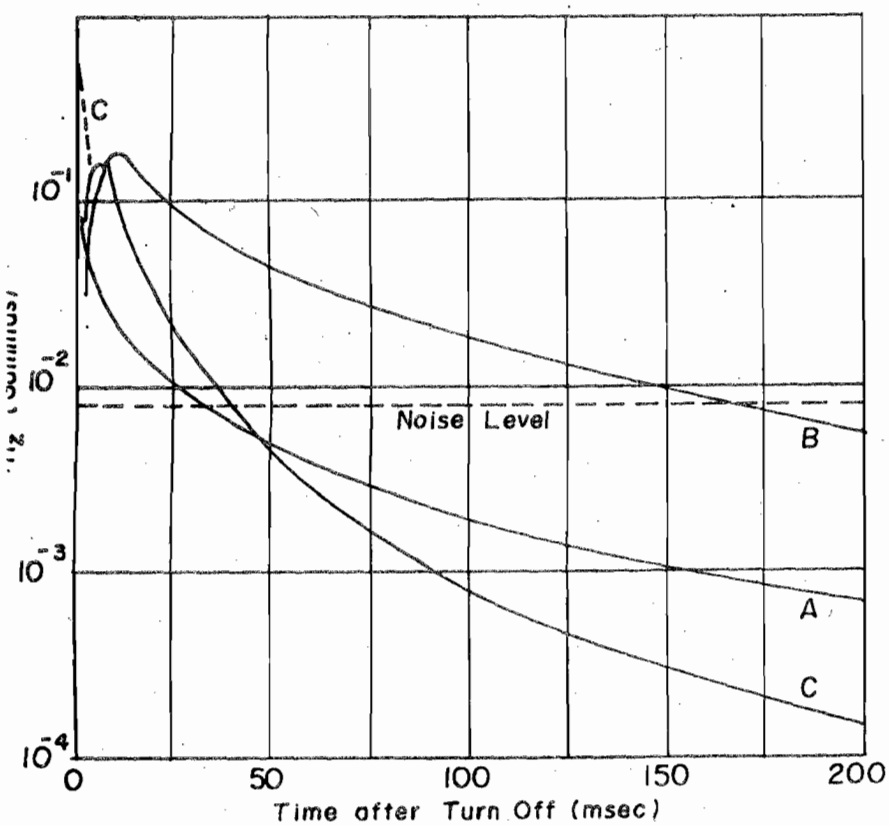

Figure12 H_r (t) 0.05-200.0 msec time interval

FEM Data

Figure 13 presents ellipticity from 1 to 20,000 hertz along with the standard errors at each frequency in the two FEM data sets.

In the low frequency band, 1 to 2000 hertz, model C requires the least averaging time and model A requires the most. If the FEM band were 1 to 100 hertz model B would be faster than C, but from 100 to 2000 hertz the model B signal is beneath the noise level, while the model C signal does not fall below the noise level until the frequency is above 8000 hertz.

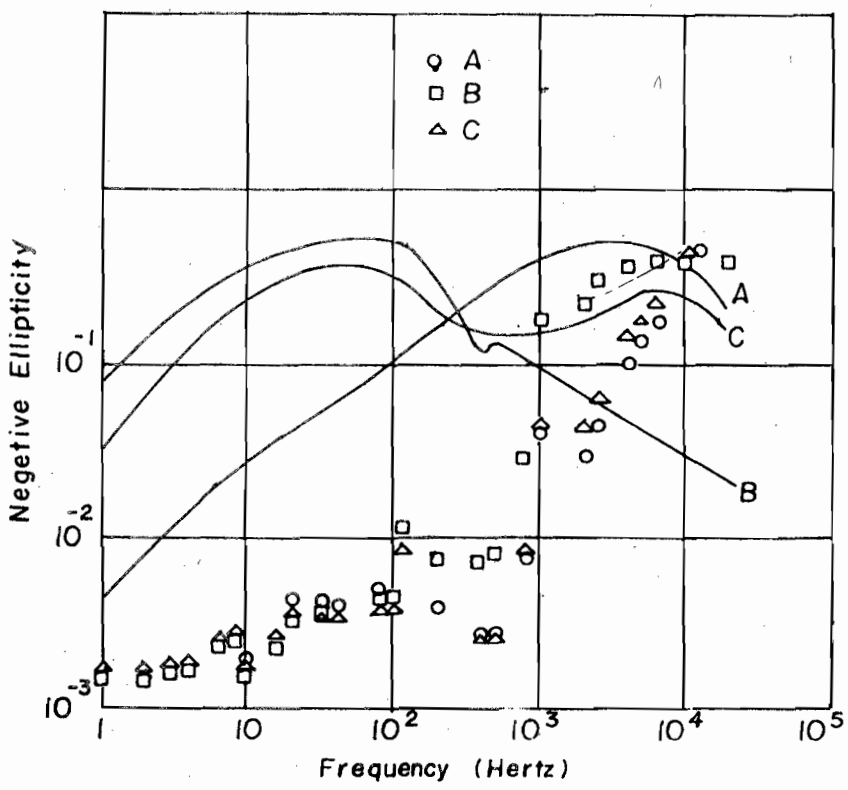

Figure 13:Ellipticity with calculated standard errors

For the high frequency band, 25 to 20,000 hertz, the order of the time required changes to A, C, B. This reflects the response characteristics of the models in that the model with the highest average resistivity has better S/N ratios at high frequencies where its response peaks.

The results of these two frequency bands illustrates the desirability of picking a data set in accordance with any apriori knowledge of the conductivity structure. It should be noted that a major source of the FEM errors at high frequencies is due to the bandwidth of the filters used. For the four-pole Butterworth filters used in the EM-60 systems the bandwidth is approximately one half of the frequency at which the filter is notched. Thus, at 10^4 hertz equation (9) shows the FEMm error is increased by a factor of 70 due solely to the filters. Newer filter design with faster roll-off characteristics would improve this source of noise. In addition, it should be noted that the FEM times quoted neglect any operational time needed in changing frequencies and associated changes in instrument settings. Actual field time for a FEM sounding would be greater.

CONCLUSION

We have considered three areas of comparison between FEM and TEM data sets. First, in terms of sensitivity to sensor coil orientation the FEM quantity ellipticity is the most insensitive to orientation error. The TEM $H_z(t)$ has orientation errors less than 1% for times after turn-off greater than 0.5 msec. Secondly, in terms of model parameter standard errors TEM and FEM data sets yield approximately the same errors for important parameters of buried conductor models such as A and C. However, for Model B, with a conductive overburden, the FEM ellipticity gave substantially better errors when compared to TEM data. Finally, in terms of the averaging times required, the TEM data with a high frequency content needed less time than the FEM high frequency data sets. While along the TEM and FEM data sets with low frequency content (0.5 to 200 msec and 1 to 2000 hertz) the averaging times for the FEM ellipticity are shorter than for either TEM quantity.

This comparison indicates that FEM ellipticity should be considered as an alternative to TEM data, particularly in conductive environments and/or for situations where low frequency information is necessary.

ACKNOWLEDGEMENT

I would like to thank the Australian Development Agency, for the award of a Commonwealth Post-graduate Fellowship to the author and the Department of geology and Geophysics, the University of Adelaide for providing physical facilities. Help and advice received from Dr. Dennis O'Brien, Dr. G. Buselli and Prof. D. M. Boyd are gratefully acknowledged.

REFERENCES

Buselli; G., 1974. Mutichannel transient electromagnetic measurements near C loncurry: CSIRO Div. Of Mineral Phys. Inv. Report no. 103.

Gleno, W. E., Ryu, J., Ward, S. H., Peeples, J. J., and Phillips, R. J., 1973. The inversion of Vertical Magnetic Dipole Sounding Data" Geophysics, 38: 1109-1129.

Glenn, W. E. and Ward, S. H., 1976. Statistical Evaluation of Electrical Sounding Methods. Part I: Experiment Design: Geophysics, 41: 1207-1221.

Hoversten, G. M. and Morrison, H. F., 1981. Transient Fields of a Current Loop Source Above a Layered Earth: Geophysics, 1982 pp. 1068 – 1077.

Inman, J. R., 1975. Resistivity Inversion with Ridge Regression: Geophysics, 40: 798-817.

Johnsen, H. K. and Sorensen K., 1979. Fast Hankel Transforms: Geophys. Prosp., 27: 876-901.

Kaufman, A. A., 1978. Frequency and Transient Responses of Electro-magnetic Fields Created by Currents in Confined Conductors: Geophysics, 43: 1002-1010.

Kaufman, A. A., 1978. Resolving Capabilities of the Inductive Methods of Electroprospecting: Geophysics, 43: 1392-1398.

Kramer, M. and Morrison, H. F., 1980. Time Domain Option for EM-60 Digital Signal Processor: "Lawrence Berkeley Laboratory Report.

Labson, V. F., 1980. Observation of Natural Audio Frequency Magnetic Field:" presented at the 50th Annual International Meeting of the Society of Exploration Geophysicists, Houston, TX.

Lee. T. and Lewis, R., 1974. Transient electromagnetic (EM) response of a large loop on layered ground. Geophy. Prospect. 22: 430 -444

Lee. T., 1982. Asymptotic expansions for transient electromagnetic fields Geophysics vol. 47: 38-46.

McCracken, K. G., Hohmann, G. W. Oristagilio, M. L., 1980. Why Time Domain?: Bull. Aust. Soc. Explor. Geophys., 11(4): 318-321.

Morrison, H. F., Goldstein, N. E., Hoversten, G. M., Opplinger, G. and Riveros, C., 1978. Description, Field Test and Data Analysis of a Controlled-Source E. M. System (EM-60): Lawrence Berkeley Laboratory Report LBL-7088 UC-666.

Oppenheim, A. V., and Schofer, R. W., 1975. Digital signal processing: new Jersey, Prentice- Hall.

Spies. B. R., 1975. the dual loop configuration of the transient electromagnetic field; Geophysics, 40: 1051-1057.

Sunde, E. O., 1949. Earth Conduction Effects in Transmission Systems: Dover Press.

Ukaigwe .N. F.,1998. Electromagnetic Method in Geoelectrical Prospecting Sherbrooke Publishers 616p.

Verma, R. V. and Mallick, K. 1979, "Detectibility of Intermediate Conductive and Resistive Layers by Time-Domain Electromagnetic Sounding:" Geophysics, 44: 1862-1877.

Ward, S. H., Smith, B. D., Glenn, W. E., Rijo, L. and Inman, J. R., 1976. Statistical Evaluation of Electrical Sounding Methods. Part II: Applied Electromagnetic Dept Sounding:" Geophysics, 41: 1222-1235.